Probabilistic Optimisation of the Maintenance of Steel Components in French Nuclear Power Facilities

Emmanuel Ardillon
EDF-R&D, PRISME Department, Chatou, France, E-mail: emmanuel.ardillon@edf.fr
Guillaume Viard
EDF/UNIE, GMAP Group, Saint-Denis, France, E-mail: guillaume.viard@edf.fr

ABSTRACT: Certain steel components located in the secondary part of PWR (Pressurized Water Reactors) nuclear power plants are subject to an atmospheric corrosion phenomenon in a confined medium affecting their bottom by the external surface. For one of them (a vessel), several campaigns to measure the thickness of the bottom of the vessel are available over time over a population of measurement points. It is possible to assess, from these measurements, a distribution of thickness loss kinetics and, at each measurement point, a distribution of residual thickness over time, and a risk of underthickness. By combining these individual risks, we obtain a global risk of underthickness over time for the entire population of measurement points. By imposing a limit on this risk, we deduce a number of points to repair.

1. INTRODUCTION

Certain structural steel components located in the secondary part of PWR (Pressurized Water Reactors) nuclear power plants are subject to an atmospheric corrosion phenomenon in a confined medium affecting their bottom by the external surface. For one of them (a vessel), several campaigns to measure the thickness of the bottom of the vessel are available over time over a population of measurement points.

These points are located in the peripheral zone of the bottom where corrosion is most active. The measurements show a significant effect of corrosion with a global decrease in thickness over time

It is possible to assess, from these measurements, a distribution of thickness loss kinetics and, at each measurement point, a distribution of residual thickness over time, and a risk of underthickness. By combining these individual risks, we obtain a global risk of underthickness over time for the entire population of measurement points. By imposing a limit on this risk, we deduce a number of points to repair.

This paper presents the detailed principle of the probabilistic approach implemented, following the steps of a usual uncertainty treatment study, as well as its main results useful for optimizing maintenance on this component.

2. GENERAL METHODOLOGICAL FRAMEWORK

2.1. General approach

This is a predictive probabilistic approach making it possible to obtain the evolution of the measured residual thickness (on which the failure criterion relates) over time. We are in a prognostic type approach. For each year to come, we are thus able to calculate at each measurement point:

- A distribution of residual thickness, real or measured;
- A risk of underthickness.

It is then possible to combine, at any given moment, these individual risk assessments to obtain a global risk of underthickness of the entire population of measurement points at a desired moment, and therefore to follow the evolution of the global risk of underthickness over time.

2.2. *Structural Reliability: general problem, R-S elementary case*

The approach presented is therefore a structural reliability approach (Lemaire, 2009). These approaches are in current use in the hydropower sector (Ardillon et al., 2022). Compared to the deterministic approach, it should be noted that the probabilistic approach has the double advantage of allowing a rigorous treatment of uncertainties, as well as a precise assessment of risk.

Let us mention that the well-known general Structural Reliability problem consists in computing the following integral:

$$P_f = \int_{D_F} f_{X_1 \dots X_n}(X_1, \dots, X_n) dX_1 \dots dX_n \quad (1)$$

where D_F is the failure domain (defined by $G(X_{i=1\dots n}) < 0$) and $(X_i)_{i=1\dots n}$ denotes the input random variables of the mechanical model G, with joint probability density $f_{X1\dots Xn}(X_1,\dots, X_n)$. They characterize the structural state, and the G-function enables to state whether this state is safe or not.

For the rest of this article, it is useful to provide some quick reminders about the well-known R-S case.

When the R and S variables are assumed to be Gaussian and independent, one gets directly an analytical expression of P_f:

$$P_f = P(R - S \leq 0) = \Phi(-\beta), \text{ with } \beta = \frac{\mu_R - \mu_S}{\sqrt{(\sigma_R^2 + \sigma_S^2)}} \quad (2)$$

where β denotes the reliability index, μ_X and σ_X denote respectively the mean and standard deviation of the variable X, and Φ the cumulative distribution function of the reduced centered normal distribution. The reliability index used here is that of Hasofer-Lind, of the FORM method (Lemaire, 2009).

3. GENERAL MODELING

3.1. *Failure criterion*

The failure criterion, in connection with the resistance of the component to earthquakes, relates to the measured thickness Th_{mes}. For points already repaired, the criterion is $Th_{mes} \leq 0$ mm, for unrepaired points, the criterion is $Th_{mes} \leq 2$ mm.

The quantity of interest is therefore the probability, at the instant considered, that the measured thickness is less than the considered threshold.

3.2. *Significance of corrosion*

This issue cannot be detailed in this paper but the use of the nonparametric statistical test of Wilcoxon, the Wilcoxon signed-rank test (Wilcoxon, 1945) for paired samples shows that statistically significant differences exist between the measured thickness distributions.

3.3. *Model selected for the evolution of the degradation phenomenon*

The available knowledge only consists of thickness measurements over time on the various measurement points monitored. We therefore naturally only have access to the evolution rate in the measured thickness. But this quantity does not directly reflect the physics of the phenomenon and its real kinetics. It is the real kinetics that is responsible of the thickness loss, and makes it possible to make a link with a possible physico-mathematical model (not available in our case). Furthermore, reasoning about the evolution rate in the measured thickness artificially increases the dispersion of the phenomenon, all the more so as the two campaigns chosen to evaluate this rate are close in time. It is therefore preferable to show the real kinetics in the model.

Second, we assume that the real loss of thickness is linear over time. This linearity assumption is valid for many corrosion phenomena of steel (Ardillon, 2013) such as flow-accelerated corrosion or corrosion of concrete reinforcements (Sudret, 2005). It is conservative for other corrosion phenomena (evolution according to t^A, where $A < 1$) (Czarnecki, 2008). Of course, the assumption of linearity, common to many corrosion phenomena and conservative in some cases, does not mean that the corrosion rates of the different phenomena are similar.

By definition of the global measurement error denoted ε, we have at any time t the relation (3):

$$Th_{mes}(t) = Th_{real}(t) + \varepsilon \quad (3)$$

Note that ε is qualified as a global measurement error (denoted GME) because, in addition to the error of the measurement process itself (ultrasound), it also includes the random error in the location of the measurement. Conventionally, it is considered to be independent of the real thickness.

We can therefore see that this example required, in the perhaps temporary absence of an adequate physical degradation model, a phase of developing the most relevant model given the available information. This is an element of originality of this study, the physical model (behavior, degradation) being often an input for structural reliability analyses.

3.4. Calculation of the real thickness loss kinetics from the evolution rate in the measured thickness

From Eq. (3) follows the following Eq. (4), which makes it possible to obtain the kinetics of real thickness loss between times t_i and t_j from the evolution rate of the measured thickness:

$$K_{ij,\,mes} = K_{ij,\,real} + (\varepsilon_j - \varepsilon_i) / (t_j - t_i) \quad (4)$$

ε_i and ε_j respectively denote the GME at times t_i and t_j ($t_j > t_i$). These are two independent and identically distributed random variables (i.i.d).

$K_{ij,\,mes}$ denotes the annual evolution rate in thickness measured between times (years) t_i and t_j.

$K_{ij,\,real}$ denotes the annual evolution kinetics of the real thickness between the times (years) t_i and t_j.

Note that with the adopted sign conventions, $K_{ij,\,mes}$ and $K_{ij,\,real}$ will generally be negative.

We see that the assumption of an unbiased error ($\mu_\varepsilon = 0$) is not necessary. On the other hand, ε is assumed to be stationary, and independent of the real thickness (but not of the measured thickness).

It follows from (4) that if the measurement error ε follows a normal law and if the evolution rate of the measured thickness also follows a normal law, then the real kinetics also follows a normal law.

Still after (4), we have the following relations (valid whatever the law of ε):

$$\mu_{ij,\,mes} = \mu_{ij,\,real} \quad (5)$$

$$\sigma^2_{ij,\,mes} = \sigma^2_{ij,\,real} + (2.\sigma^2_\varepsilon) / (t_j - t_i)^2 \quad (6)$$

$\mu_{ij,\,mes}$ (resp. $\mu_{ij,\,real}$) denote the mean of $K_{ij,\,mes}$ (resp. of $K_{ij,\,real}$)

$\sigma^2_{ij,\,mes}$ (resp. $\sigma^2_{ij,\,real}$) denote the variance of $K_{ij,\,mes}$ (resp. of $K_{ij,\,real}$)

σ^2_ε denotes the variance of the global measurement error (GME).

It can be seen that the variability of the real kinetics is systematically lower than that of the evolution rate of the measured thickness. The difference is all the greater the shorter the time interval, as mentioned in paragraph 3.3. The estimation of $\sigma^2_{ij,\,real}$ therefore requires knowledge of the GME characteristics; its estimation will be all the more robust with respect to this parameter as the evaluation period of the kinetics will be long.

3.5. Expression of the limit state function G: calculation of the residual thickness measured at each measurement point over time

To evaluate the thickness measured at point k at the instant $t_i > t_0$ from the thickness measurement available at t_0, it is necessary:

• Return to the real thickness distribution at point k at t_0, by "subtracting" a measurement error;

• Add the real loss of thickness over the time interval [t_0; t_i]: we thus obtain the real thickness distribution at point k at time t_i;

• Add a measurement error to obtain the thickness distribution measured at point k at time t_i.

This is expressed through the following Eq. (7):

$$Th_{mes,k}(t_i) = Th_{mes,k}(t_0) - \varepsilon_0 + c_{0i,\,real}\,.\,(t_i - t_0) + \varepsilon_i \quad (7)$$

$Th_{mes,k}$ (t_i) (resp. $Th_{mes,k}$ (t_0)) denotes the thickness measured at point k at time t_i (resp. t_0).

As already said, variables ε_0 and ε_i are i.i.d. We can therefore reduce to a single random variable noted ε', with zero mean and variance equal to $2.\sigma^2_\varepsilon$. ε_0 and ε_i being assumed to be Gaussian, ε' is also Gaussian.

It is therefore a problem with 2 independent random variables (the state vector $X = (K_{0i,\,real}, \varepsilon')$). And the limit state function G of the problem (for an individual measurement point) writes:

$$G(X) = G(K_{0i,\,real}, \varepsilon') = Th_{mes,k}(t_0) + K_{0i,\,real}\,.\,(t_i - t_0) + \varepsilon' - Lim \quad (8)$$

Lim is the thickness threshhold (equal to 2mm).

We are therefore brought back to the basic case R-S (cf. §2.2), with the following correspondance:

$$R = Th_{mes,k}(t_0) + \varepsilon' - Lim \quad (9)$$

$$S = K_{0i,\,real}\,.\,(t_i - t_0) \quad (10)$$

R represents the GME contribution, S represents the contribution of the kinetics.

3.6. *Quantities of interest*

These are mainly:

- The evolution of the individual risk of underthickness over time at each measurement point;
- The evolution of the global risk of underthickness over time over the entire population of measurement points.

4. UNCERTAINTY QUANTIFICATION

4.1. *Applied approach*

It is necessary to estimate the joint distribution of the state random vector ($K_{0i,\ real}$, ε'), consisting of 2 obviously independent random variables.

4.1.1. *ε' variable*

It is known to have a zero mean. This amounts to identifying the marginal law of ε. Classically, for a measurement error, a normal distribution is considered. It remains to evaluate its standard deviation. This is done by expert judgement, and also in coherence with the measurement data. Indeed, Eq. (6) of §3.4 shows that one necessarily has:

$$\sigma_{ij,\ mes} \, . \, (t_j - t_i) \, / \, \sqrt{2} \geq \sigma_\varepsilon \qquad (11)$$

which gives an upper bound of σ_ε.

4.1.2. *Corrosion rate $K_{0i,\ real}$*

First, it should be noted that the available data are related to $K_{0i,\ mes}$, not directly to $K_{0i,\ real}$, that is the input variable of interest.

Here, unlike ε', it is hardly expert judgement because data is available. It is necessary to choose the evaluation period (i.e. between which measurement campaigns). On the selected data, a first normality test must then be performed to see if the normality assumption is acceptable, and then a distribution must be chosen based on the results of the usual fit or model selection tests.

The normality test chosen is the Shapiro-Wilk test (Saporta, 2006). It is the most recommended normality test (Saporta, 2006); indeed, it is considered the most powerful of these tests for small samples (i.e. < 50 values) (Rakotomalala, 2011).

It is well known that the fit and model selection tests rarely give similar results in terms of distribution ranking. Therefore a set of available tests has been considered for this analysis. They are those available in Persalys version 5. These are the Kolmogorov-Smirnov test and the Bayesian Information Criterion (BIC). Both tests are used. They have been complemented by a visual analysis of the Q-Q plot (theoretical vs. empirical quantiles plot), and also by consistency criteria (e.g. for the support of $K_{0i,\ mes}$ that should be infinite according to Eq. (4)). These statistical goodness-of-fit tests are shortly presented in (D'Agostino, 1986) or in the documentation of the OpenTURNS software (Baudin, 2017).

The Kolmogorov-Smirnov (KS) goodness-of-fit test is probably the most popular goodness-of-fit test at least in the structural reliability community. However, this study was an opportunity to realize that the KS test is in fact not appropriate in our context. Indeed, the KS test is valid for comparing distributions whose parameters do not come from an estimate on the sample considered, but from another source of information. In our case (as perhaps in the majority of goodness-of-fit analyses performed in structural reliability), the parameters are directly estimated from the sample. The appropriate test in this case is the Lilliefors test (Lilliefors, 1967). But, for practical reasons of computation time and convergence, this Lilliefors test is not implemented for the moment in Persalys. It was available at the time of the study in OpenTURNS, but at the price of practical difficulties which since then seem to have been solved (Version 1.16, November 2020), precisely thanks to an interaction with this study. These two tests give quite different p-values, but it is possible that they lead to similar rankings. This comparison could not yet be made in this study.

4.2. Numerical results

4.2.1. *Variable ε'*

As seen previously, ε' follows a normal centered distribution with standard deviation equal to $\sigma_\varepsilon . \sqrt{2}$. As mentioned in §4.1.1, we can identify an upper bound of σ_ε: for one of the campaign couples, we find that σ_ε must be less than 0.31.

In the end, the hypotheses = 0.2 and = 0.3 will be tested.

4.2.2. Corrosion rate $K_{0i, real}$

The fits actually relate to $K_{0i, mes}$: the available data are thickness measurements. One then returns to real kinetics by formulas (5) to (7) of §3.4.

4.2.2.1 Available data

Four measurement campaigns are available: 2001, 2010, 2012, 2016. 12 thickness measurements are available for campaign 2001, 23 for campaigns 2010 to 2016.

4.2.2.2 Campaign selection

It was decided to favor the distribution of kinetics from the 2001 to 2016 campaigns. The main reason is to make the results more robust to GME. Indeed, as mentioned in §3.4 above, the uncertainty associated with the GME has an impact that is all the greater on the evolution rate of the mesured thickness $K_{0i, mes}$ as the measurement instants are close. As a result, in the reverse direction, the real kinetics distribution will be less sensitive to assumptions about GME for spaced measurement instants. This can be seen by testing two hypotheses: $\sigma_\varepsilon = 0.2$ mm and $\sigma_\varepsilon = 0.3$ mm, σ_ε denoting the standard deviation of the GME.

4.2.2.3 First justification of distribution normality for $K_{0i, mes}$

The test used is the Shapiro-Wilk normality test.

In addition to checking the normality of $K_{0i, mes}$, we also check that of the thickness distributions in 2001 and 2016, since these 3 variables are linked by a linear relationship: if 2 of them are Gaussian, the 3rd one must be too. This issue cannot be developed in this paper. It is shown that all the distributions can be assumed to be normal.

4.2.2.4 Goodness-of-fit to data: selection of the normal distribution for $K_{0i, mes}$

A list of 18 distirbutions available in Persalys is considered in the goodness-of-fit analysis.

In terms of goodness-of-fit, the results show that no distribution gives systematically better results than the normal distribution. In particular, the normal distribution:

- is acceptable for the BIC (Bayesian Information Criterion);
- gives good results for the non-parametric Kolmogorov-Smirnov test;
- leads to the best QQ-plot;
- has an infinite support consistent with the GME distribution.

We therefore decide to adopt the normal distribution.

The corresponding estimated parameters (mean and standard deviation) are (in mm):

$\mu = -0.0628$; $\sigma = 0.0411$.

4.2.2.5 Distribution for $K_{0i, real}$

So, both distributions of $K_{0i, mes}$ and ε' are normal, and $K_{0i, mes}$ and ε' are independent. Consequently, the distribution of $K_{0i, real}$ is also normal (Meister, 2009).

Note that if both distributions of $K_{0i, mes}$ and ε' were not normal, the determination of $K_{0i, real}$ distribution would be a complex deconvolution problem with generally no exact parametric distribution solution.

Its parameters can be derived from Eqs. (5) and (6): $\mu_{0i, real} = -0.0628$ mm, and $\sigma_{0i, real}$ depends on σ_ε, and is given in the Table 1 below.

Table 1 : Values of the standard deviation of $K_{0i, real}$

σ_ε**(mm)**	0.3	0.2
$\sigma_{ij, real}$ **(mm)**	0.0299	0.0366

These results confirm the relative insensitivity of $\sigma_{0i, real}$, to the variability of GME. The preferred hypothesis is $\sigma_\varepsilon = 0.3$mm.

Moreover, we will notice that the real kinetics distribution is necessarily negative, which is not completely the case with the normal distribution we arrive at. However, given the values of $\mu_{0i, real}$ and $\sigma_{0i, real}$, this truncation would only affect about 2% of the distribution. The impact of truncation would then likely be (very) small on the results. Computations with the truncated normal distribution (not described in this paper) confirm that it is the case. It was therefore decided to keep the normal law not truncated.

5. UNCERTAINTY PROPAGATION

5.1. Applied approach

5.1.1. Individual underthickness risk: reliability index, underthickness probability under Gaussian assumption

ε’ following a normal (Gaussian) distribution, this is also the case for R defined in paragraph 3.5 (Eq. (9)). If we assume that the kinetics are normal, S is normal and according to Eq. (2), we can evaluate the reliability index, the failure probability and the corresponding sensitivity factors. Applying the formulas gives:

$P_f = \Phi(-\beta)$, with

$$\beta = \frac{Ep_{mes,k}(t_0) - \text{seuil} - \mu_{0i,réel}.(t_i - t_0)}{\sqrt{(2.\sigma_\varepsilon^2 + \sigma_{0i,réel}^2.(t_i - t_0)^2)}} \qquad (12)$$

5.1.2. Evolution of the global underthickness risk for the population of all measurement points

We note $P_f(t_i, k)$ the underthickness risk at the measurement point k and at the instant t_i.

It comes :

$$P_f(t_i, k) = P[Th_{mes,k}(t_i) < Lim]$$

$$= P(G(c_{0i,\,real}, \varepsilon') < 0) \qquad (13)$$

By assuming the "underthickness" events of each measurement point to be mutually independent (assumption applicable to the case studied and conservative when there is a positive correlation of certain events), we obtain the global risk of underthickness at time t_i, RG (t_i) by cumulating the individual risks of the n measurement points as follows:

$$RG(t_i) = 1 - \prod_{k=1}^{n}(1 - P_f(t_i, k)) \qquad (14)$$

This is the probability, at the instant t_i, that there is at least 1 point among the n measurement points in underthickness.

It should be noted that this global risk has an upper bound, which is also valid with or without the independence assumption mentioned above. One gets:

$$RG(t_i) \le RG_{sup}(t_i) = \sum_{k=1}^{n} P_f(t_i, k) \qquad (15)$$

$RG(t_i)$ and $RG_{sup}(t_i)$ are close if $RG_{sup}(t_i) << 1$

In addition, we also have an evaluation of the average number of points in underthickness (noted N^{moy}_{uth}) at time t_i; it just so happens to be the upper bound above:

$$N^{moy}_{uth} = \sum_{k=1}^{n} P_f(t_i, k) \qquad (16)$$

Moreover, a sensitivity analysis can be carried out and shows that the relative importance of the variables on the underthickness risk depends only on the ratio of the quantities $\sigma_{0i,réel}.(t_i - t_0)$ and $\sqrt{2}.\sigma_\varepsilon$ (less than, equal to or greater than 1).

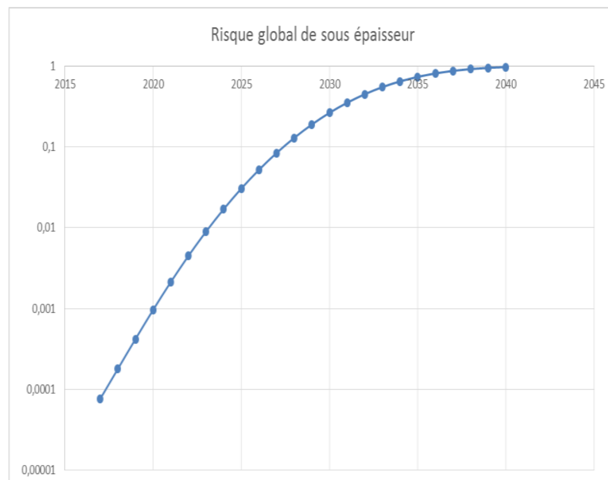

Figure 1. Global underthickness risk as a function of time

5.2. Numerical results

As the individual risks of each measurement point are ultimately an intermediary result, they are not given in this article.

The global risk is calculated on the population of the 23 measurement points, using the formulas in §5.1.3 (global risk).

Figure 1 shows the evolution of the global risk over time, up to 2040 (σ_ε = 0.3 mm).

First of all, it appears that the global risk in 2023 remains very low (0.9%). Without maintenance intervention, the global risk in 2033 is between 54.8% (σ_ε = 0.3 mm) and 58.6% (σ_ε = 0.2 mm). The variability of the global measurement error therefore has little impact on the result.

In addition, it also appears that even without intervention, the average number of points in underthickness remains nevertheless lower than 1 in

2033: one has $N^{moy}_{uth} = 0.76$. This number may seem low.

6. USE OF PROBABILISTIC RESULTS: DETERMINATION OF THE POINTS TO BE REPAIRED

6.1. Applied approach

Here we describe how the global risk assessments from the previous steps of the approach are used.

The criterion considered is the global risk of underthickness in 2033, $RG(t_i = 2033)$.

If $RG(t_i = 2033)$ exceeds 10%, we will look for the minimum set of n_p measurement points to repair (patch). This helps to minimize the repairs to be made. This set corresponds to the points of greatest individual risk, classified by decreasing risk, by retaining only the 1st points allowing to reach a global risk less than or equal to 10%. In other words, we then select n_p points such as:

$$RG_{n\backslash np}(t_j = 2033) < 10\% \text{ and}$$
$$RG_{n\backslash np+1}(t_j = 2033) \geq 10\%) \qquad (17)$$

In a 2nd phase of the study, the level of tolerated risk was taken equal to 5%. This also makes it possible to take into account the modeling assumptions and in particular the fact that the samples used for the adjustment of the distribution of thickness loss kinetics are small.

It should be noted that the risk levels adopted do not of course correspond to a risk of failure under normal operating conditions, but to a risk of exceeding the “failure” criterion, sized for the earthquake, at at least one measurement point.

It is also interesting to have an evaluation of the average number of points in underthickness (N^{moy}_{uth}) at time t_j, but this is not a criterion.

6.2. Numerical results

The number of points to be repaired depends on the global risk criterion adopted. As seen previously, it was initially set at 10%. We will therefore select the points to be repaired sequentially, starting from the point of greatest individual risk and removing them as the contribution to the global risk progresses until it drops below 10%. For the unrepaired points, these are of course the points with the lowest measured thickness in 2016.

In total, the points to be repaired before 2033 are:

- 1 point already repaired in 2016;
- 7 points not repaired in 2016.

By repairing them, we reach a global risk of only 8.5%.

The average number of points in underthickness having removed the repaired points would then be 0.089 in 2033, which is very low.

If we want to reduce the risk to only 5%, then two more points must be repaired; the global risk is then 5.03%. For the risk to be strictly less than 5%, you have to repair a 3rd additional point and the global risk is then 4.04%.

In any case, it appears that it is not necessary to replace the bottom of the component, it is sufficient to repair some points (8 to 11).

7. CONCLUSION

Certain structural steel components located in the secondary part of PWR nuclear power plants are subject to atmospheric corrosion in a confined environment affecting their bottom through the external surface. For one of them (it is a vessel), several campaigns of thickness measurements of the bottom of the vessel are available over time on a population of measurement points identified in the peripheral zone of the bottom, the most sensitive to corrosion.

It is possible to evaluate, from these measurements, a distribution of thickness loss kinetics and, at each measurement point, a residual thickness distribution over time, and a risk of underthickness. By cumulating these individual risks, we obtain a global risk of underthickness over time. By imposing a limit on this risk, we deduce a number of points to repair (patch).

<u>Industrial interest</u>

First of all, compared to the deterministic approach, it appeared that the probabilistic approach has the double advantage of allowing a rigorous treatment of uncertainties (rather than a stacking of margins with conservatism not always controlled), as well as a precise risk assessment.

Considering the year 2033 as a time horizon, we find that without maintenance intervention, the global risk in 2033 is between 54.8% (σ_ε = 0.3 mm) and 58.6% (σ_ε = 0.2 mm). The variability of the measurement error therefore has little impact on the result.

In the end, if we accept a global risk of underthickness of 10% in 2033 (decision criterion), it is necessary to repair 8 points out of the 23, which are the 8 points of greatest individual risk. 7 are new points to repair, 1 is a point already repaired. If we consider a risk of 5%, we must repair 2 or 3 additional points.

It is therefore not necessary to proceed with the complete replacement of the bottom, local repairs (by laying patches) on a certain number of points resulting from the study are sufficient to guarantee the fitness-for-service of the equipment. This contributes to a significant optimization of its corrective maintenance.

These results are currently being used internally. They may be accompanied by additional calculations (sensitivity study). The recommended maintenance interventions should take place in the years to come.

Scientific interest

Structural reliability has demonstrated its ability to solve an industrial problem, even in its most elementary form (R-S case). It is clear that the R-S case is not a purely academic example.

In the absence of an adequate physical degradation model, this study included a first phase of model development, based in the available information (thickness measurements). This is an element of originality of this study, the physical model (behavior, degradation) being often an input data of structural reliability analyses.

The study will also have confirmed the need to be able to assess a global risk (union of events) and therefore to process system events. This point was recently (2019) integrated to OpenTURNS, which since version 1.14 allows to calculate probabilities of system events. It will therefore have confirmed the relevance of this evolution of the software. It will also have shown the need to have sensitivity indices for these probabilities of system events.

8. REFERENCES

Agostino, R.B. d', Stephens, M.A. (1986). *Goodness-of-fit techniques*, Marcel Dekker.

Ardillon, E. (2013). Time-variant structural reliability: some theoretical considerations for industrial practice. *Proceedings of the 11th Conference on Structural Safety and Reliability*, New York, USA

Ardillon, E., Bryla, P. & Dumas, A. (2022). Penstock reliability assessments: some results and developments. *Proceedings of the 13th Conference on Structural Safety and Reliability*, Shanghai, China

Baudin, M., Dutfoy, A., Iooss, B. & Popelin, A.-L. (2017). OpenTURNS: An industrial software for uncertainty quantification in simulation. In: Handbook of uncertainty quantification, R. Ghanem, D. Higdon and H. Owhadi (Eds), Springer. HAL version - Springer link

Czarnecki, A. & Nowak, A. (2008). Time-variant reliability profiles for steel girder bridges. *Structural Safety* 30: 49-64.

Lemaire, M. (2009). *Structural Reliability*. Ed. by Jacky Mazars. London: ISTE Ltd., Wiley

Lilliefors, H.M. (1967). On the Kolmogorov-Smirnov Test for Normality with Mean and Variance Unknown. *Journal of the American Statistical Association, Vol. 62, No 318, pp. 399-402*

Meister, A. (2009). *Deconvolution problems in non parametric statistics*. ISBN 978-3-540-87556-7, Springer-Verlag, Berlin, Heidelberg

Rakotomalala, R. (2011). Tests de normalité: techniques empiriques et tests statistiques. On line document, Université Lumière Lyon 2.

Rawal, P., Pang, W., & Pei, B. (2017). Selection of probability distributions to represent simulated hurricane wid data and its applications, *Proceedings of the 12th International Conference on Structural Safety and Reliability*, Vienna, Austria

Rocquigny, E. de, Devictor, N. & Tarantola, S. (2008). *Uncertainty in Industrial Practice – A Guide to Quantitative Uncertainty Management*. London: ISTE Ltd., Wiley

Saporta, G. (2006). *Probabilités, Analyse des Données et Statistique*, 2nd edition, Technip.

Sudret, B., Defaux, G. & Pendola, M. (2005). Time-variant finite element reliability analysis – application to the durability of cooling towers. *Structural Safety* 27: 93-112.

Wilcoxon, F. (1945). Individual Comparisons by Ranking Methods, *Biometrics Bulletin*, Vol. 1, pp. 80-83